Analysis of the electron self-energy for tightly bound electrons

Ingvar Lindgren, Hans Persson, Sten Salomonson, and Per Sunnergren
Department of Physics, Chalmers University of Technology and Göteborg University, S-41296 Göteborg, Sweden
(Received 24 June 1997; revised manuscript received 3 February 1998)

A general scheme for mass renormalization of the electron self-energy in strong nuclear fields is developed. In second order the results agree with those recently obtained by Labzowsky and Mitrushenkov [Phys. Rev. A **53**, 3029 (1996)], and, in particular, it is shown that the extra counterterm observed by these authors appears quite naturally in the more general scheme developed here. [S1050-2947(98)08407-8]

PACS number(s): 31.30.Jv, 31.10.+z

I. INTRODUCTION

Considerable progress has recently been made in measuring the hyperfine structure and Lamb shift of low-Z systems, such as hydrogen, positronium, muonium, and helium atoms. Corresponding progress has been made in the theoretical development, and a remarkable agreement between theory and experiment has in most cases been achieved [1,2]. The calculations on these systems are carried out by means of the $Z\alpha$ expansion of the nuclear field, Z being the nuclear charge and α the fine-structure constant.

Recently, considerable progress has also been made in measuring the level shift (Lamb shift) of highly charged ions [3]. The Lamb shift of the $1s$ level of hydrogenlike uranium, for instance, has been measured by Beyer *et al.* [4] to be 470 ± 16 eV, relative to the Dirac value for a point nucleus. This experimental result can be well explained theoretically by considering the effect of the finite nucleus and the first-order (one-photon) *quantum electrodynamical*, QED, correction, which can now be calculated with high accuracy [5]. Experiments are in progress, however, for reducing the uncertainty, hopefully below the 1-eV level. As discussed in a recent paper [6], the second-order QED contributions, as well as nuclear recoil and nuclear polarization effects, will then be of significance.

The Feynman diagrams for the second-order (two-photon) QED shift in hydrogenlike ions are shown in Fig. 1. The first line (a,b,c) of the figure represents the double vacuum polarization (VP-VP), the second line (d,e,f) the combined vacuum-polarization self-energy contributions (SE-VP), and the third line (g,h,i) the second-order self-energy contributions (SE-SE).

At strong nuclear fields, the $Z\alpha$ expansion is no longer applicable, and numerical all-order techniques have to be applied. Here, the basic electron orbitals are generated in the field of the nucleus—and in some cases also of the inner electrons. Such techniques have been developed and employed during the last ten years [5–16]. Specifically, the VP-VP and SE-VP contributions have all been calculated numerically (a) by Persson *et al.* [7], (b,c) by Beier and Soff and by Schneider *et al.* [8], (d,e) by Lindgren *et al.* [9], and (f) by Persson *et al.* [6] and by Mallampalli and Sapirstein [10]. It should be noted that diagrams (c,f) have only been calculated in the Uehling approximation. The SE-SE contributions (g,h,i) in Fig. 1, on the other hand, have not yet been calculated by numerical techniques, and the analysis of this part forms the main subject of the present investigation. Since these effects should be about a factor of α smaller than the first-order self-energy effects, they can be expected to be of the order of 1–2 eV.

In order to evaluate the higher-order self-energy contributions, it is necessary to reconsider the renormalization procedure. This will be done in the present paper in a way that is easily generalized to arbitrary order. In a recent publication by Labzowsky and Mitrushenkov [17] the second-order problem has been considered and an expression is derived for the corresponding energy shift. The treatment of Labzowsky and Mitrushenkov is based on the potential-interaction expansion of the bound-state orbitals, which is the standard procedure for treating the first-order self-energy. In the second-order case, this leads to a rather lengthy derivation, and the procedure can hardly be generalized beyond that order. In the present paper we shall analyze the mass renormalization in a more general way, which will lead to a procedure for generating renormalized self-energy expressions that can more easily be extended to higher orders. Second-order expressions, identical to those of Labzowsky

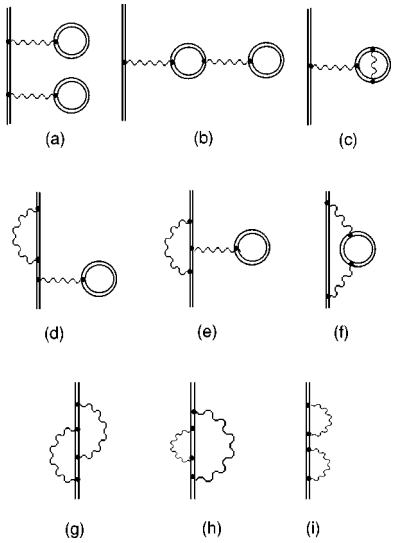

FIG. 1. The second-order Lamb-shift diagrams for a single-electron system. The double lines represent orbitals and propagators generated in the nuclear field. The first row of diagrams (a,b,c) represents the double vacuum polarization (VP-VP), the second row (d,e,f) the combined self-energy vacuum-polarization (SE-VP), and the last row (g,h,i) the second-order self-energy (SE-SE).

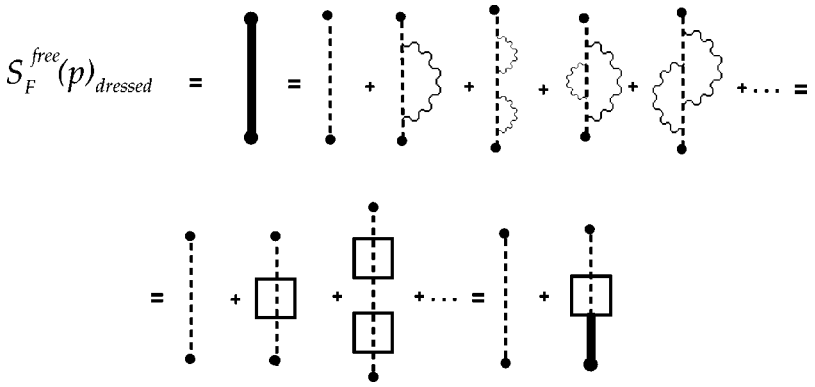

FIG. 2. The dressed electron propagator is represented by the bare electron propagator with all possible SE insertions. This can be expressed as a Dyson equation by means of the *proper* SE diagrams, represented by the square box. Note that all internal lines inside the self-energy diagrams are *bare electron lines*, represented by dotted lines.

and Mitrushenkov, are presented.

The main purpose of the present paper is to analyze the mass-renormalization procedure for higher-order self energies, particularly at strong external fields. For that reason we start in Sec. II by analyzing the free-electron self-energy and the free-electron propagator in a general way, starting from the bare electron mass. Dressing the free-electron propagator by self-energies in all possible ways, leads to the dressed free-electron propagator, and—after mass renormalization—this propagator is expressed as the propagator of the *physical* electron, dressed with *mass-renormalized* self-energies. This yields a recursive renormalization scheme, which can easily be extended to higher orders. In Sec. III the treatment is extended to electrons in external electrical (nuclear) fields, and in Sec. IV general expressions for the corresponding energy shift are given, using energy-dependent perturbation theory. Explicit expressions for the diagrams involved in second order are given in Appendix C. The question of numerical evaluation is not considered in any detail in the present paper. However, one part of the second-order (SE-SE) has been calculated numerically by Mitrushenkov *et al.* [18] and very recently some additional parts have been calculated by Mallampalli and Sapirstein [19].

II. FREE ELECTRONS

We start by analyzing the free-electron propagator, and we use the following *operator form*:

$$\hat{S}_F(\omega)=\frac{1}{\omega-\hat{h}(1-i\eta)}=\sum_t \frac{|t\rangle\langle t|}{\omega-E_t(1-i\eta)},$$

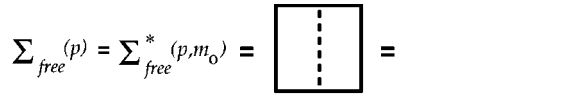

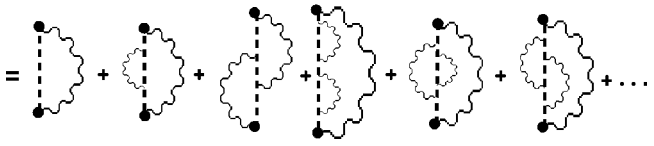

FIG. 3. The proper free-electron self-energy is given by all proper free-electron self-energy diagrams, with the internal lines associated with the *bare* electron mass.

where $\hat{h}$ is the single-electron Hamiltonian, and $|t\rangle$ and E_t are the corresponding eigenfunctions and eigenvalues. Insertion of all possible self-energy operators into the electron propagator, leads to the ''*dressed*'' propagator (for simplicity leaving out the infinitesimal imaginary part)

$$\hat{S}_F(\omega)_{dressed}=\frac{1}{\omega-\hat{h}+\Sigma(\omega)}. \tag{2.1}$$

Here, $\Sigma(\omega)$ denotes the *proper* self-energy (SE) operator, represented by all SE diagrams that cannot be separated into two allowed diagrams by cutting a single-electron line. This implies, for instance, that the diagrams (g,h) in Fig. 1 are proper SE diagrams, while diagram (i) is not.

We consider now a *free electron* with the ''*bare*'' mass m_0 (with no electromagnetic self-interactions), which is represented by the Hamiltonian (using relativistic units, $\hbar=c=\epsilon_0=1$, $e^2=4\pi\alpha$)

$$\hat{h}^{free}(m_0)=\boldsymbol{\alpha}\cdot\hat{\mathbf{p}}+\beta m_0.$$

The free-electron propagator in operator form is then

$$\hat{S}_F^{free}(\omega,m_0)=\frac{1}{\omega-\boldsymbol{\alpha}\cdot\hat{\mathbf{p}}-\beta m_0}, \tag{2.2}$$

with the Fourier transform (see Appendix A)

$$S_F^{free}(\omega,\mathbf{p},m_0)=\frac{1}{\omega-\boldsymbol{\alpha}\cdot\mathbf{p}-\beta m_0}, \tag{2.3}$$

or in covariant form

$$S_F^{free}(p,m_0)=\frac{1}{\not{p}-m_0}\beta. \tag{2.4}$$

(This differs from the standard definition by a factor of β, because we base the definition on using $\psi^\dagger$ rather than $\bar{\psi}$.)

The interaction with the electromagnetic field gives rise to all possible SE interactions, as indicated in Fig. 2. This leads to the ''*dressed*'' *free-electron propagator*

$$S_F^{free}(p)_{dressed}=\frac{1}{\not{p}-m_0+\beta\Sigma_{free}(p)}\beta, \tag{2.5}$$

which can also be expressed by means of a Dyson equation, illustrated in the bottom line of Fig. 2. The *proper free-*

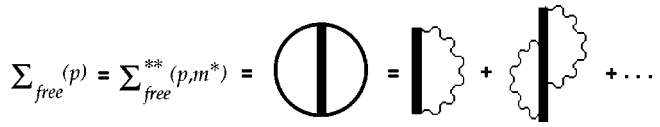

FIG. 4. The proper free-electron self-energy can also be expressed as the sum of all self-energy *skeletons*, represented by the circle, with fully dressed internal lines, represented by heavy solid lines (cf. Fig. 2).

electron self energy is denoted by $\Sigma_{free}(p)$ and is represented by the sum of all proper, free-electron SE diagrams with the internal lines associated with the unphysical, *bare* electron mass m_0 ,

$$\Sigma_{free}(p)=\Sigma^{*}_{free}(p,m_0),$$

as illustrated in Fig. 3.

The free-electron SE exhibits two kinds of divergences, which we refer to as the mass and the charge divergence, respectively. The mass divergence is eliminated by means of the mass renormalization, which is the main issue of the present paper. The charge divergence of the SE is canceled by the corresponding divergence of the vertex modification (Ward identity [20]). In performing the renormalization, a proper regularization scheme has to be employed. At this stage we shall not make any specific choice of regularization scheme, although it will be assumed in the following—when needed—that all quantities are properly regularized.

A. Renormalization

The dressed electron propagator (2.5) should have the same pole positions as the propagator of the *physical* electron with the mass m,

$$S_F^{free}(p,m)=\frac{1}{\not p-m}\beta,$$

i.e., at $\not p=m$. This implies that

$$|\Sigma_{free}(p)|_{\not p=m}=|\Sigma^{*}_{free}(p,m_0)|_{\not p=m}=\beta(m_0-m)=-\beta\delta m.$$

Instead of working with the bare mass m_0, we can use the *physical* mass m, and introduce a *mass counterterm* into the Hamiltonian,

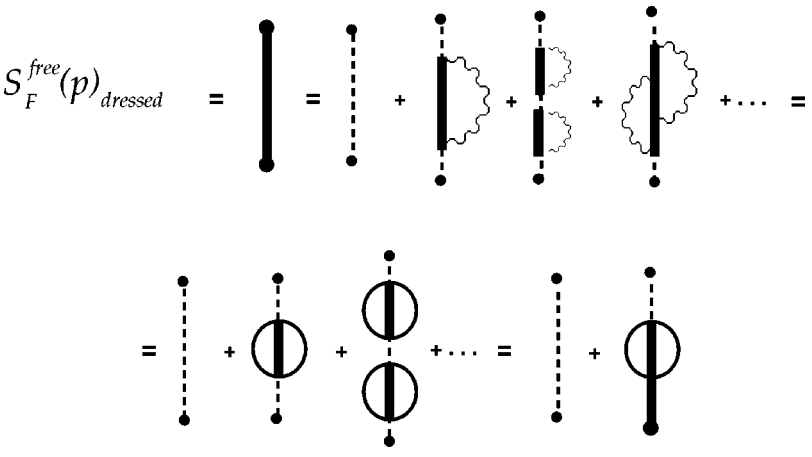

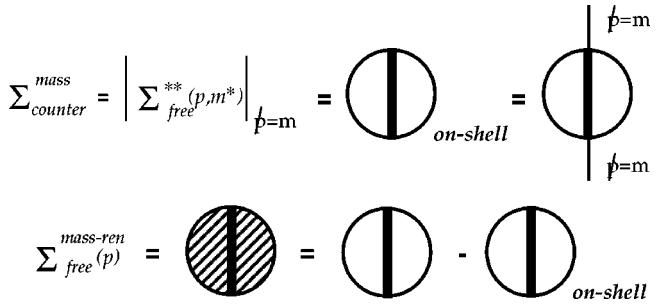

FIG. 5. The mass counterterm is given by all free-electron self-energy skeletons with fully dressed internal lines, evaluated *on the mass shell*, $\not p=m$. The *mass*-renormalized free-electron self-energy is obtained by subtracting the mass counterterm from the free-electron self-energy, displayed in Fig. 4.

$$\Sigma^{mass}_{counter}=|\Sigma_{free}(p)|_{\not p=m}=|\Sigma^{*}_{free}(p,m_0)|_{\not p=m}=-\beta\delta m. \tag{2.6}$$

This leads to the *mass-renormalized* free-electron SE,

$$\Sigma^{mass\text{-}ren}_{free}(p)=\Sigma_{free}(p)-\Sigma^{mass}_{counter},$$

and the dressed, free-electron propagator (2.5) can alternatively be expressed

$$S_F^{free}(p)_{dressed}=\frac{1}{\not p-m+\beta\Sigma^{mass\text{-}ren}_{free}(p)}\beta. \tag{2.7}$$

After proper regularization, the free-electron SE can be expanded around $\not p=m$,

$$\Sigma_{free}(p)=A+(\not p-m)B+(\not p-m)^2C(p),$$

where A and B are constants,

$$A=|\Sigma_{free}(p)|_{\not p=m}=-\beta\delta m$$

and

$$B=\left|\frac{\partial}{\partial\not p}\Sigma_{free}(p)\right|_{\not p=m}.$$

$C(p)$ is finite for $\not p=m$ and associated with the *mass*- and *charge-renormalized free-electron* SE, $\Sigma^{ren}_{free}(p)$,

FIG. 6. The (charge-unrenormalized) dressed electron propagator in Fig. 2 can also be obtained from the *bare* electron propagator by inserting all SE *skeletons* with *dressed* internal lines [see Eqs. (2.5) and (2.8)].

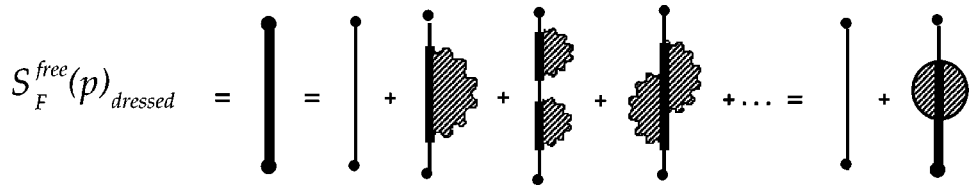

FIG. 7. The dressed, free-electron electron propagator in Fig. 6 can also be obtained from the undressed, *physical* free-electron propagator by inserting all *mass-renormalized* SE skeletons (shaded) with dressed internal lines [see Eqs. (2.7) and (2.10)]. The procedures represented by Figs 5 and 7 have to be carried out recursively in higher orders.

$$(\not{p}-m)^2 C(p)=\Sigma_{free}^{ren}(p)=\Sigma_{free}^{mass\text{-}ren}(p)-(\not{p}-m)B.$$

It should be noted that the dressed, free-electron propagators in the form of Eq. (2.7) is free from mass divergence, since it has been *mass* renormalized. The *charge* divergence, on the other hand, is still present due to the B term of the SE, and this will be further analyzed in Appendix D.

B. Skeletons

We shall find it convenient in the following to work with *skeleton* diagrams. A skeleton is defined as a proper SE diagram that cannot be obtained from another SE diagram by modifying an internal electron line by an SE insertion. This implies, for instance, that diagram (g) in Fig. 1 is a skeleton, while diagram (h) is not. (The latter can be obtained from the first-order diagram by an SE insertion.) From this definition it follows that all proper SE diagrams either are skeletons or can be obtained from skeletons by (successive) modifications by SE insertions on electron lines. It is also obvious that all such modifications of skeletons lead to allowed, proper SE diagrams. A systematic way of generating all proper SE diagrams is therefore to insert successively—starting with the skeletons—new skeletons on internal lines of the diagrams in all possible ways. All internal lines of the diagrams will then be fully dressed. This is the procedure we shall adopt in the following.

It should be noted that we consider here only modifications of the *electron* lines. This implies that with this definition vertex modifications will lead to new skeletons. In principle, also polarization insertions on the photon lines will lead to new skeletons. In the present paper, however, we shall not consider modifications of photon lines. In principle, such effects, after proper renormalization, could also be included in the procedure presented here.

It follows from the above that the free-electron SE, given by all proper free-electron SE diagrams, can also be expressed as the sum of *all skeletons* with *fully dressed* internal lines

$$\Sigma_{free}(p)=\Sigma_{free}^{**}(p,m^*), \tag{2.8}$$

as illustrated in Fig. 4. Σ_{free}^{**} represents here all SE skeletons, and m^* indicates that all internal lines are fully dressed. We can then express the mass counterterm (2.6) as

$$\Sigma_{counter}^{mass}=|\Sigma_{free}^{**}(p,m^*)|_{\not{p}=m}. \tag{2.9}$$

Thus, the mass counterterm equals the sum of all free-electron SE skeletons with fully dressed electron lines, evaluated on the mass shell, $\not{p}=m$, as is illustrated schematically in the upper part of Fig. 5. We then obtain the final form of the mass-renormalized free-electron SE that we shall employ in the following:

$$\Sigma_{free}^{mass\text{-}ren}(p)=\Sigma_{free}^{**}(p,m^*)-|\Sigma_{free}^{**}(p,m^*)|_{\not{p}=m}. \tag{2.10}$$

This is illustrated in a schematic way in the bottom part of Fig. 5.

In order to apply the expression (2.10), we need a way of evaluating the fully dressed (charge-unrenormalized) electron propagator. This is defined as the bare electron propagator with all possible self-energy insertions with bare internal lines, but, of course, we need to reexpress this in terms of the propagator of the *physical* electron. For that reason we first express the fully dressed electron propagator as the bare

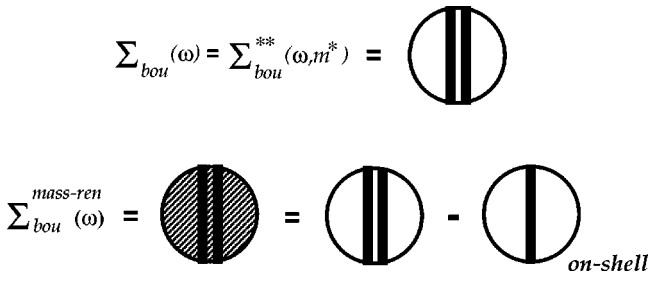

FIG. 8. The (unrenormalized) bound-state self-energy is given by all bound-state self-energy skeletons with dressed internal lines [see Eq. (3.1)]. The mass renormalization is obtained by removing the mass counterterm [see Eqs. (3.3) and (2.8) and Fig. 5]. The shaded area represents, as before, the mass renormalization. The fat double line represents here the dressed bound-state propagator and the fat single line, as before, the dressed free-electron propagator.

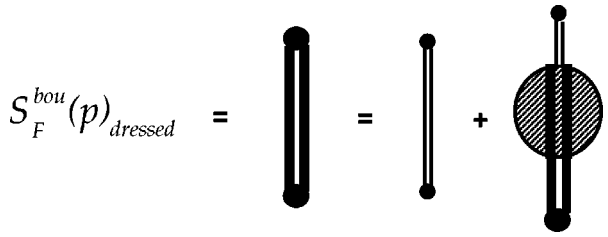

FIG. 9. The dressed bound-state electron propagator, Eq. (3.2), can be obtained from the undressed (physical) bound-state propagator by inserting all *mass-renormalized* self-energy skeletons with fully dressed internal lines, in analogy with the free-electron case illustrated in Fig. 7. The thin (fat) double line represents the undressed (dressed) bound-state propagator. As in the free-electron case (Fig. 7) the relations in Figs. 8 and 9 have to be treated recursively.

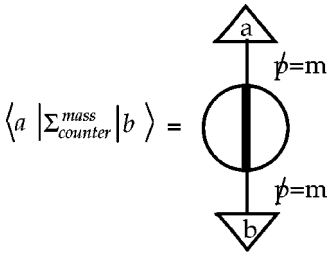

FIG. 10. The mass counterterm is, according to Eq. (2.9) and Fig. 5, given by all free-electron skeletons with dressed internal lines, evaluated on the mass shell. Its matrix elements between bound states Eq. (4.2) can be evaluated by expressing these states in the momentum representation (here represented by the triangles).

electron propagator, dressed with all *skeletons* with *dressed* internal lines, using Eq. (2.8) and illustrated in Fig. 6. After renormalization, this can be expressed as the *physical* electron propagator dressed with all *renormalized* skeletons with dressed internal lines, according to Eq. (2.7) and illustrated in Fig. 7. Obviously, the procedure of dressing and renormalization, illustrated in Figs. 5 and 7, has to be carried out *recursively*. This is of vital importance and has important consequences, as we shall demonstrate below.

III. ELECTRONS IN EXTERNAL FIELD

In treating atomic electrons, moving in the field of the nucleus, the standard procedure is to start from free electrons and use the nuclear field as a perturbation. In order to avoid the double perturbation expansion, we define here a ''bound-state'' electron propagator, using electron orbitals generated in the nuclear field. The electron propagator associated with the bare mass, m_0 , then becomes

$$\hat{S}_F^{bou}(\omega,m_0)=\frac{1}{\omega-\hat{h}^{bou}(m_0)}=\sum_{t_0}\frac{|t_0\rangle\langle t_0|}{\omega-E_{t_0}^{bou}},$$

where

$$\hat{h}^{bou}(m_0)=\boldsymbol{\alpha}\cdot\hat{\mathbf{p}}+\beta m_0+V$$

is the external-field or *''bound-state''* Hamiltonian. V is the external (nuclear) field, $|t_0\rangle$ represents the eigenstates of $\hat{h}^{bou}(m_0)$ (in the following referred to as ''*bound*'' states), and $E_{t_0}^{bou}$ represents the corresponding eigenvalues. [In the bound case we shall find it more convenient to work with the *operator* form, Eqs. (2.1) and (2.2), of the propagator rather than the Fourier transform, used in the free-electron case, Eqs. (2.3) and (2.4).]

The interaction with the electromagnetic field gives rise to all possible self-energy insertions, as in the free-electron case. According to Eq. (2.1) this leads to the *dressed bound-state electron propagator* [cf. Eq. (2.5)]

$$\hat{S}_F^{bou}(\omega)_{dressed}=\frac{1}{\omega-\hat{h}^{bou}(m_0)+\Sigma_{bou}(\omega)},$$

where $\Sigma_{bou}(\omega)=\Sigma_{bou}^{*}(\omega,m_0)$ is the *proper bound-state self-energy operator*, represented by all proper bound-state SE diagrams, with the internal electron lines associated with bound electrons with the *bare* mass m_0. This propagator is represented by the same diagrams as the free-electron propagator in Fig. 2, with the dotted lines now representing *bound* states (still with the *bare* electron mass m_0). As in the free-electron case, the bound-state SE can also be represented by all bound-state SE skeletons with fully dressed internal lines

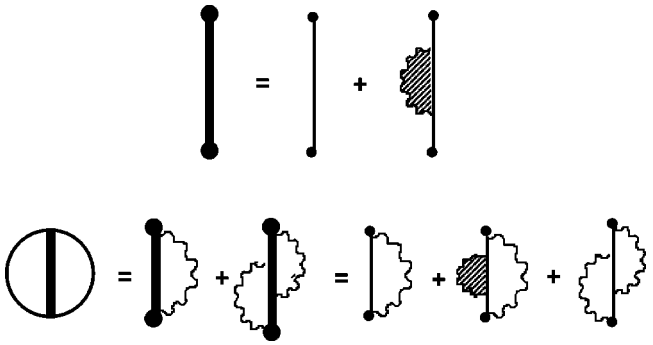

FIG. 11. Expansion of the dressed free-electron propagator to first order (cf. Fig. 7) and the free-electron self-energy to second order.

$$\Sigma_{bou}(\omega)=\Sigma_{bou}^{**}(\omega,m^*),\tag{3.1}$$

as illustrated in Fig. 8 (upper part) (cf. Fig. 4). The fat double line represents here the fully dressed bound-state propagator.

By introducing the *mass counterterm* (2.6), we can express the (charge-unrenormalized) dressed bound-state electron propagator in analogy with Eq. (2.7) as

$$\hat{S}_F^{bou}(\omega)_{dressed}=\frac{1}{\omega-\hat{h}^{bou}(m)+\Sigma_{bou}^{mass\text{-}ren}(\omega)},\tag{3.2}$$

where $\Sigma_{bou}^{mass\text{-}ren}(\omega)$ is the *mass-renormalized bound-state self-energy* operator. Using Eqs. (3.1) and (2.8), this becomes

$$\begin{aligned}\Sigma_{bou}^{mass\text{-}ren}(\omega)&=\Sigma_{bou}(\omega)-\Sigma_{counter}^{mass}\\&=\Sigma_{bou}^{**}(\omega,m^*)-|\Sigma_{free}^{**}(p,m^*)|_{\not p=m},\end{aligned}\tag{3.3}$$

which is illustrated in the bottom part of Fig. 8.

The fully dressed, bound-state propagator can then be represented as shown in Fig. 9 in complete analogy with the free-electron case in Fig. 7; i.e., by inserting all *mass-renormalized* bound-state self-energy skeletons with fully

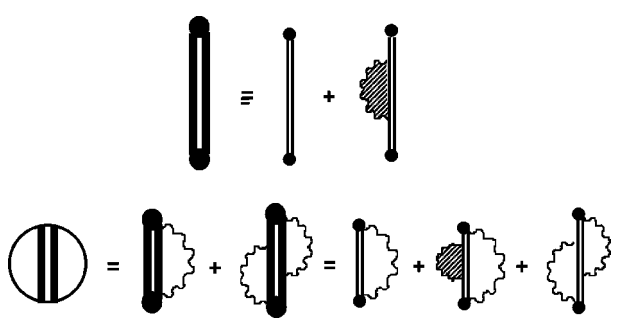

FIG. 12. Same as Fig. 11 for bound states.

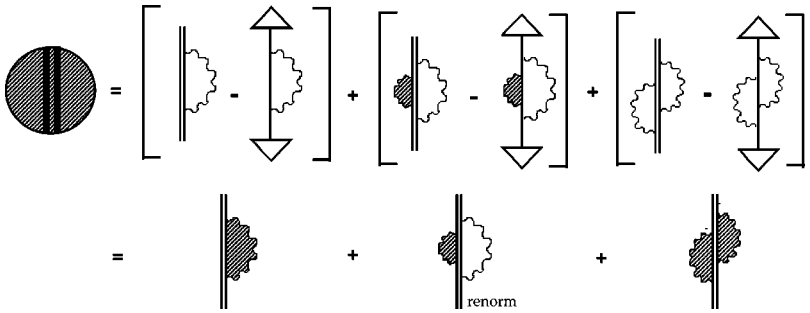

FIG. 13. Expansion of the mass-renormalized proper bound-state self-energy to second order. The renormalization terms are defined in Fig. 10 and Eq. (4.2).

dressed internal bound-state lines. Again, of course, the dressing and renormalization procedures have to be carried out *recursively*.

IV. EXPRESSION FOR THE SELF-ENERGY SHIFT

In the present section we shall outline a general procedure for evaluating the energy shift of an external-field or ''bound'' state due to the SE, which is the major radiative correction. This shift is given by the shift in the pole position, corresponding to the state considered, of the dressed propagator (3.2). The pole positions are given by the eigenvalues of the operator $\hat{h}^{bou}(m)-\Sigma_{bou}^{mass\text{-}ren}(\omega)$. $\Sigma_{bou}^{mass\text{-}ren}(\omega)$ can here be regarded as an *energy-dependent* perturbation, and we get the shift by applying the expressions for energy-dependent perturbation theory [21], derived in Appendix B. The energy shift of the unperturbed bound state $|a\rangle$ with the unperturbed energy E_a is then given by

$$\Delta E_a=\langle a|-\Sigma_{bou}^{mass\text{-}ren}(E_a)|a\rangle+\sum_{E_t\neq E_a}\frac{\langle a|-\Sigma_{bou}^{mass\text{-}ren}(E_a)|t\rangle\langle t|-\Sigma_{bou}^{mass\text{-}ren}(E_a)|a\rangle}{E_a-E_t}$$
$$+\cdots+\langle a|-\Sigma_{bou}^{mass\text{-}ren}(E_a)|a\rangle\left\langle a\left|\left\{\frac{\partial}{\partial\omega}[-\Sigma_{bou}^{mass\text{-}ren}(\omega)]\right\}_{\omega=E_a}\right|a\right\rangle+\cdots, \tag{4.1}$$

where the last term represents the *reference-state contribution* ($E_t=E_a$) [9].

In order to evaluate the expression (4.1), we first have to interpret the quantity

$$\langle a|\Sigma_{bou}^{mass\text{-}ren}(E_a)|b\rangle=\langle a|\Sigma_{bou}(E_a)-\Sigma_{counter}^{mass}|b\rangle,$$

where the mass counterterm is given by Eq. (2.9). The latter should be evaluated on the *free-electron mass shell*, and for that reason we expand the bound-state states in the momentum representation

$$\langle a|\Sigma_{counter}^{mass}|b\rangle=\sum_{\mathbf{p}\mathbf{p}'rr'}\langle a|\mathbf{p},r\rangle\langle\mathbf{p},r|\Sigma_{counter}^{mass}|\mathbf{p}'r'\rangle\langle\mathbf{p}'r'|b\rangle, \tag{4.2}$$

where $\mathbf{p}$ represents the three-dimensional momentum and r the spinor state. The matrix element of the mass counterterm is represented graphically in Fig. 10, where the triangles represent the expansion of the bound state in free-electron states.

In second order the formula (4.1) yields

$$\Delta E_a^{(2)}=\langle a|-\Sigma_{bou}^{mass\text{-}ren(2)}(E_a)|a\rangle+\sum_{E_t\neq E_a}\frac{\langle a|-\Sigma_{bou}^{mass\text{-}ren(1)}(E_a)|t\rangle\langle t|-\Sigma_{bou}^{mass\text{-}ren(1)}(E_a)|a\rangle}{E_a-E_t}$$
$$+\langle a|-\Sigma_{bou}^{mass\text{-}ren(1)}(E_a)|a\rangle\left\langle a\left|\left\{\frac{\partial}{\partial\omega}[-\Sigma_{bou}^{mass\text{-}ren(1)}(\omega)]\right\}_{\omega=E_a}\right|a\right\rangle, \tag{4.3}$$

where $\Sigma_{bou}^{mass\text{-}ren(1)}$ and $\Sigma_{bou}^{mass\text{-}ren(2)}$ represent the mass-renormalized first- and second-order proper self-energies, respectively. The second and third terms of Eq. (4.3) correspond to the ''irreducible'' (nondegenerate) and ''reducible'' (degenerate) parts, respectively, of the improper second-order SE [cf. the diagram (i) in Fig. 1]. The last term of Eq. (4.3) can also be obtained by applying the Gell-Mann–Low–Sucher formula [22] to that diagram in combination with the (singular) disconnected second-order diagram.

In order to find a graphical representation of the mass-renormalized SE to second order, we apply the recursion procedure outlined above. Using the expansion in Fig. 7, the dressed free-electron propagator is to second order represented by the diagrams in Fig. 11 (upper part), and using Fig.

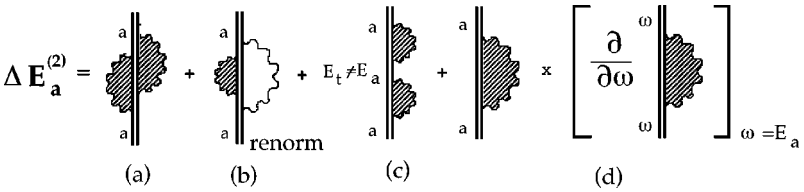

FIG. 14. Graphical representation of the second-order energy shift due to the self-energy interaction, given by Eq. (4.3). The shaded parts represent mass-renormalized SE diagrams, displayed in more detail in Fig. 13.

4 this leads to the corresponding free-electron SE, given in the lower part of that figure. The corresponding expansion in the bound case is given in Fig. 12. The mass-renormalized SE is obtained by removing the mass counterterm, i.e., the matrix element of the on-shell free-electron SE according to Eqs. (2.9) and (4.2). Using the notations of Fig. 10, this leads to the diagrammatic representation in Fig. 13 of the first- and second-order mass-renormalized SE, $\Sigma_{bou}^{mass\text{-}ren(1)}$ and $\Sigma_{bou}^{mass\text{-}ren(2)}$, evaluated in the bound state $|a\rangle$.

The complete graphical representation of the second-order energy contribution is obtained by adding the representation of the last two terms of Eq. (4.3). This is exhibited in Fig. 14.

In order to see the identity of our results with those of Labzowsky and Mitrushenkov (LM) [17] in more detail, we can replace the renormalized first-order SE on the internal lines in the second set of brackets of Fig. 13 by the unrenormalized first-order SE minus the corresponding mass counterterm, as shown in the first set of brackets of the same figure. This leads to a graphical representation that is identical to that of LM. In particular, we can see that the ''extra'' terms observed by LM appear quite naturally in our procedure.

In principle, the scheme described here can be extended to arbitrary order. Applying the recursive schemes displayed in Figs. 5 and 7 for the free electrons and in Figs. 8 and 9 for the bound electrons yields the expansion of the self-energy to successively higher orders. Insertion in the general perturbation scheme, generated according to the principles shown in Appendix B, then yields the expansion of the corresponding energy shift.

The analytical expressions corresponding to the second-order diagrams are given in Appendix C. There we have chosen to perform the z integration explicitly (for positive intermediate states). These expressions are fully equivalent to those of LM, the only difference being that LM have performed the k integration explicitly.

Several of the individual terms of the energy expression are infrared as well as ultraviolet divergent, although the entire expression is finite. For the numerical evaluation the various contributions have to be regularized, e.g., by the Pauli-Villars procedure or by dimensional regularization. In first order it is found that the partial-wave expansion works without any further regularization. This is not generally the case, as we have recently demonstrated [23]. In the present paper we are not particularly concerned with the numerical evaluation. This will be addressed in a forthcoming paper, where the regularization procedure has to be considered in more detail.

The main purpose of the present paper has been to develop a general procedure for the mass renormalization of the self-energies to arbitrary order. The conventional potential expansion of the bound-state wave functions and propagators is largely avoided. It is believed that the generalized procedure gives some additional insight into the mass renormalization. In second order, our results are shown to be identical to those recently derived by Labzowsky and Mitrushenkov, using the potential-expansion method.

ACKNOWLEDGMENTS

Financial support was provided by the Swedish Natural Science Research Council (NFR) and the Knut and Alice Wallenberg Foundation. The authors wish to acknowledge stimulating discussions with Leonti Labzowsky and Gerhard Soff.

APPENDIX A: FREE-ELECTRON PROPAGATOR

In this appendix we collect, for convenience, various formulations of the free-electron propagator, which are used in the main text. The free-electron propagator in the *operator form* is

$$\hat{S}_F^{free}(\omega)=\frac{1}{\omega-\hat{h}^{free}(1-i\eta)}=\sum_{\mathbf{p},r}\frac{|\mathbf{p},r\rangle\langle\mathbf{p},r|}{\omega-E_{\mathbf{p},r}(1-i\eta)},$$

where $\hat{h}^{free}$ is the Dirac Hamiltonian *operator* for a free particle

$$\hat{h}^{free}=\boldsymbol{\alpha}\cdot\hat{\mathbf{p}}+\beta m,$$

with the eigenfunctions in discrete and continuous case, respectively,

$$\langle\mathbf{x}|\mathbf{p},r\rangle=\frac{1}{\sqrt{V}}\mathbf{u}_r(\mathbf{p})e^{i\mathbf{p}\cdot\mathbf{x}}\Rightarrow(2\pi)^{-3/2}\mathbf{u}_r(\mathbf{p})e^{i\mathbf{p}\cdot\mathbf{x}}.$$

Here $r=1,2,3,4$, represents different spinor states, and the corresponding eigenvalues are denoted by $E_{\mathbf{p},r}$.

In the *coordinate representation* the free-electron propagator becomes

$$S_F^{free}(\mathbf{x}',\mathbf{x},\omega)=\langle\mathbf{x}'|\hat{S}_F^{free}(\omega)|\mathbf{x}\rangle=\sum_{\mathbf{p},r}\frac{\langle\mathbf{x}'|\mathbf{p},r\rangle\langle\mathbf{p},r|\mathbf{x}\rangle}{\omega-E_{\mathbf{p},r}(1-i\eta)}.$$

This can also be expressed

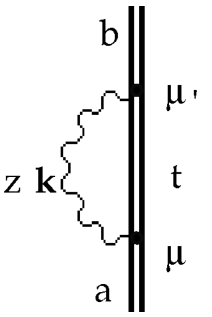

FIG. 15. First-order self-energy.

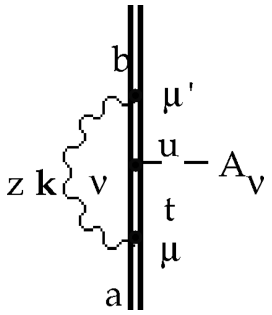

FIG. 16. Vertex correction of first-order self-energy.

$$S_F^{free}(\mathbf{x}',\mathbf{x},\omega)$$

$$=\sum_{\mathbf{p},r}\langle\mathbf{x}'|\frac{1}{\omega-h^{free}(\mathbf{p})(1-i\eta)}|\mathbf{p},r\rangle\langle\mathbf{p},r|\mathbf{x}\rangle$$

$$\Rightarrow(2\pi)^{-3}\int d^3p\sum_r\frac{e^{i\mathbf{p}\cdot(\mathbf{x}'-\mathbf{x})}}{\omega-h^{free}(\mathbf{p})(1-i\eta)}\mathbf{u}_r(\mathbf{p})\mathbf{u}_r^\dagger(\mathbf{p})$$

$$=(2\pi)^{-3}\int d^3p\frac{e^{i\mathbf{p}\cdot(\mathbf{x}'-\mathbf{x})}}{\omega-h^{free}(\mathbf{p})(1-i\eta)}, \tag{A1}$$

using

$$\sum_r \mathbf{u}_r(\mathbf{p})\mathbf{u}_r^\dagger(\mathbf{p})=\mathbf{I}(4\times4).$$

Here, $h^{free}(\mathbf{p})$ is the Dirac Hamiltonian *function* for a free particle

$$h^{free}(\mathbf{p})=\boldsymbol{\alpha}\cdot\mathbf{p}+\beta m.$$

The *momentum representation* of the free-electron propagator is

$$S_F^{free}(\mathbf{p}'r',\mathbf{p}r,\omega)=\delta_{\mathbf{p}',\mathbf{p}}\delta_{r',r}\frac{1}{\omega-E_{\mathbf{p},r}(1-i\eta)}.$$

It follows from Eq. (A1) that the *Fourier transform* of the coordinate representation of the free-electron propagator is

$$\frac{1}{\omega-h^{free}(\mathbf{p})(1-i\eta)}=S_F^{free}(\omega,\mathbf{p}).$$

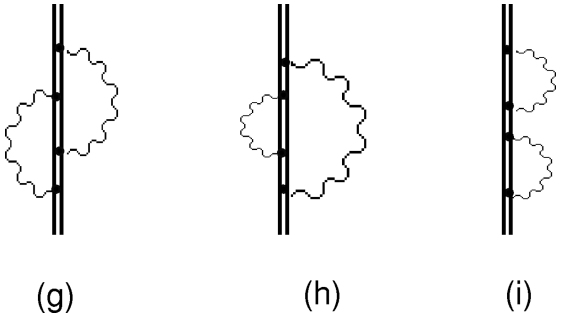

FIG. 17. Second-order self-energy.

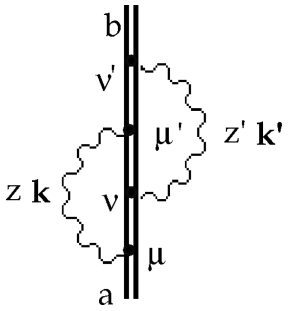

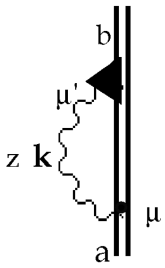

FIG. 18. Reduction of the diagram 17(g).

This can be written in covariant form (leaving out the imaginary part)

$$S_F^{free}(\omega,\mathbf{p})=\frac{1}{\omega-\boldsymbol{\alpha}\cdot\mathbf{p}-\beta m}=\frac{1}{\not p-m}\beta,$$

where with our notations $\not p=\beta(p_0-\boldsymbol{\alpha}\cdot\mathbf{p})$.

APPENDIX B: ENERGY-DEPENDENT PERTURBATION

We want to find the energy eigenvalues of the Hamiltonian

$$H'=H+V(E),$$

where $V(E)$ is an energy-dependent perturbation and the eigenvalues and eigenfunctions of H are known:

$$H\phi_i=E\phi_i. \tag{B1}$$

We assume that H is Hermitian and that the set of eigenfunctions $\{\phi_k\}$ is orthonormal. We consider in particular the energy corresponding to the unperturbed state $|a\rangle=\phi_a$ and want to solve the eigenvalue equation

$$[H+V(E_a+\delta E)](\phi_a+\delta\phi)=(E_a+\delta E)(\phi_a+\delta\phi).$$

In view of Eq. (B1) this leads to

$$(H-E_a)\delta\phi+[V(E_a+\delta E)-\delta E](\phi_a+\delta\phi)=0. \tag{B2}$$

We assume for simplicity that the unperturbed state $|a\rangle=\phi_a$ is *nondegenerate*. In *intermediate normalization*, $\langle\phi_a|\phi_a+\delta\phi\rangle=\langle\phi_a|\phi_a\rangle=1$, we can then make the expansion

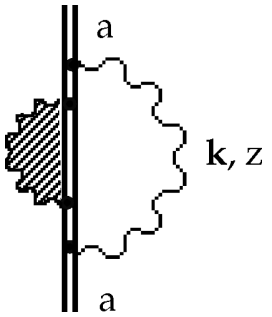

FIG. 19. Self-energy modified electron propagator.

$$\delta\phi=\sum_{k\neq a} c_k\phi_k, \quad c_k=\langle\phi_k|\delta\phi\rangle.$$

Operating on Eq. (B2) with $\langle\phi_i|$ from the left,

$$\langle\phi_i|H-E_a|\delta\phi\rangle=\langle\phi_i|\delta E-V(E_a+\delta E)|\phi_a+\delta\phi\rangle$$

gives for $i=a$

$$\langle\phi_a|\delta E-V(E_a+\delta E)|\phi_a+\delta\phi\rangle=0$$

or

$$\delta E=\langle\phi_a|V(E_a+\delta E)|\phi_a+\delta\phi\rangle \tag{B3}$$

and for $i\neq a$

$$(E_i-E_a)c_i=\delta E c_i-\langle\phi_i|V(E_a+\delta E)|\phi_a+\delta\phi\rangle$$

or

$$c_i=\frac{\langle\phi_i|V(E_a+\delta E)|\phi_a+\delta\phi\rangle}{E_a+\delta E-E_i}. \tag{B4}$$

In expanding $V(E_a+\delta E)$ and $1/(E_a+\delta E-E_i)$ in Taylor series, we can write the expressions (B3) and (B4) as

$$\delta E=\langle\phi_a|V(E_a+\delta E)|\phi_a+\delta\phi\rangle=\langle\phi_a|V(E_a)|\phi_a\rangle+\delta E\left\langle\phi_a\left|\left(\frac{\partial V}{\partial E}\right)_{E=E_a}\right|\phi_a\right\rangle+\frac{1}{2}(\delta E)^2\left\langle\phi_a\left|\left(\frac{\partial^2 V}{\partial E^2}\right)_{E=E_a}\right|\phi_a\right\rangle+\cdots$$

$$+\langle\phi_a|V(E_a)|\delta\phi\rangle+\delta E\left\langle\phi_a\left|\left(\frac{\partial V}{\partial E}\right)_{E=E_a}\right|\delta\phi\right\rangle+\cdots$$

and

$$c_i=\frac{\langle\phi_i|V(E_a+\delta E)|\phi_a+\delta\phi\rangle}{E_a+\delta E-E_i}$$

$$=\frac{\langle\phi_i|V(E_a)|\phi_a\rangle}{E_a-E_i}+\delta E\frac{\left\langle\phi_i\left|\left(\frac{\partial V}{\partial E}\right)_{E=E_a}\right|\phi_a\right\rangle}{E_a-E_i}+\frac{\langle\phi_i|V(E_a)|\delta\phi\rangle}{E_a-E_i}-\delta E\frac{\langle\phi_i|V(E_a)|\phi_a\rangle}{(E_a-E_i)^2}+\cdots.$$

An order-by-order expansion then yields

$$\delta E^{(1)}=\langle a|V(E_a)|a\rangle,$$

$$c_i^{(1)}=\frac{\langle i|V(E_a)|a\rangle}{E_a-E_i},$$

$$\delta E^{(2)}=\sum_{i\neq a}\langle a|V(E_a)|i\rangle c_i^{(1)}+\delta E^{(1)}\left\langle a\left|\left(\frac{\partial V}{\partial E}\right)_{E=E_a}\right|a\right\rangle$$

$$=\sum_{i\neq a}\frac{\langle a|V(E_a)|i\rangle\langle i|V(E_a)|a\rangle}{E_a-E_i}+\langle a|V(E_a)|a\rangle\left\langle a\left|\left(\frac{\partial V}{\partial E}\right)_{E=E_a}\right|a\right\rangle,$$

$$c_i^{(2)}=\sum_{j\neq a}\frac{\langle i|V(E_a)|j\rangle}{E_a-E_i}c_j^{(1)}-\delta E^{(1)}\frac{\langle i|V(E_a)|a\rangle}{(E_a-E_i)^2}+\delta E^{(1)}\frac{\left\langle i\left|\left(\frac{\partial V}{\partial E}\right)_{E=E_a}\right|a\right\rangle}{E_a-E_i},$$

$$\delta E^{(3)}=\frac{1}{2}(\delta E^{(1)})^2\left\langle a\left|\left(\frac{\partial^2 V}{\partial E^2}\right)_{E=E_a}\right|a\right\rangle+\sum_{i\neq a}\langle a|V(E_a)|i\rangle c_i^{(2)}+\sum_{i\neq a}\delta E^{(1)}\left\langle a\left|\left(\frac{\partial V}{\partial E}\right)_{E=E_a}\right|i\right\rangle c_i^{(1)}+\delta E^{(2)}\left\langle a\left|\left(\frac{\partial V}{\partial E}\right)_{E=E_a}\right|a\right\rangle,$$

$$\vdots$$

For an *energy-independent* perturbation, all derivative terms vanish, and we retrieve the standard Rayleigh-Schrödinger perturbation expansion.

APPENDIX C: EVALUATION OF TWO-PHOTON SELF-ENERGIES

In this appendix we shall derive analytical expressions for the second-order self-energy. For completeness we start by deriving the expression for the first-order self-energy, used in our previous works [13,15]. It should be noted that, since most expressions involved here are divergent, some scheme of regularization has to be employed. We shall not consider that any further here, but we shall assume in the following that, when needed, the expressions are properly regularized.

1. First-order

a. Self-energy

The first-order self-energy (see Fig. 15) is in the operator form represented by

$$i\Sigma^{(1)}(\omega)=\int\frac{dz}{2\pi}ie\alpha^{\mu'}iS_F(\omega-z)ie\alpha^{\mu}iD_{F\mu'\mu}(z),$$

where S_F and $D_{F\mu'\mu}$ represent the electron and photon propagators, respectively. The Feynman amplitude between the states a and b, which can be free states or bound states (generated in an external potential) is given by ($E_a=E_b$)

$$M=\langle b|i\Sigma^{(1)}(E_a)|a\rangle.$$

The corresponding energy contribution is

$$E=iM-(\text{mass counterterm}).$$

Using the Feynman gauge and relativistic units, $\hbar=c=\epsilon_0=1$, $e^2=4\pi\alpha$, the photon and electron propagators are in the coordinate representation

$$\langle\mathbf{x}_2|D_{F\nu\mu}(z)|\mathbf{x}_1\rangle=-g_{\nu\mu}\int\frac{d^3k}{(2\pi)^3}\frac{e^{-i\mathbf{k}\cdot(\mathbf{x}_2-\mathbf{x}_1)}}{z^2-\mathbf{k}^2+i\eta},$$

$$\langle\mathbf{x}_2|S_F(\omega)|\mathbf{x}_1\rangle=\sum_t\frac{\langle\mathbf{x}_2|t\rangle\langle t|\mathbf{x}_1\rangle}{\omega-E_t+i\eta_t},$$

where η_t has the same sign as the electron energy E_t. This gives the coordinate representation of the mass-unrenormalized first-order self-energy operator

$$\langle\mathbf{x}_2|i\Sigma^{(1)}_{bou}(\omega)|\mathbf{x}_1\rangle=-4\pi\alpha\int\frac{dz}{2\pi}\int\frac{d^3k}{(2\pi)^3}\sum_t\frac{\alpha_\mu e^{-i\mathbf{k}\cdot\mathbf{x}_2}|t\rangle\langle t|e^{i\mathbf{k}\cdot\mathbf{x}_1}\alpha^\mu}{(\omega-z-E_t+i\eta_t)(z^2-\mathbf{k}^2+i\eta)},$$

and after the z integration

$$\langle\mathbf{x}_2|i\Sigma^{(1)}_{bou}(\omega)|\mathbf{x}_1\rangle=2\pi\alpha i\int\frac{d^3k}{(2\pi)^3}\frac{1}{k}\sum_t\frac{\alpha_\mu e^{-i\mathbf{k}\cdot\mathbf{x}_2}|t\rangle\langle t|e^{i\mathbf{k}\cdot\mathbf{x}_1}\alpha^\mu}{\omega-E_t-k\ \mathrm{sgn}(E_t)}.$$

The corresponding energy contribution then becomes

$$\Delta E^{(1)}_{SE}=i\langle a|i\Sigma^{mass\text{-}ren(1)}_{bou}(\omega)|a\rangle=\langle a|-\Sigma^{(1)}_{bou}(\omega)|a\rangle-\langle a|-\Sigma^{mass(1)}_{counter}|a\rangle, \tag{C1}$$

where

$$\langle a|-\Sigma^{(1)}_{bou}(\omega)|a\rangle=-2\pi\alpha\int\frac{d^3k}{(2\pi)^3}\frac{1}{k}\sum_t\frac{\langle a|\alpha_\mu e^{-i\mathbf{k}\cdot\mathbf{x}}|t\rangle\langle t|e^{i\mathbf{k}\cdot\mathbf{x}}\alpha^\mu|a\rangle}{\omega-E_t-k\ \mathrm{sgn}(E_t)},$$

and using Eqs. (2.9) and (4.2)

$$\langle a|-\Sigma^{mass(1)}_{counter}|a\rangle=-2\pi\alpha\int\frac{d^3k}{(2\pi)^3}\frac{1}{k}\sum_{\mathbf{p},r}\sum_{\mathbf{p}',r'}\sum_{\mathbf{q},s}\frac{\langle a|\mathbf{p},r\rangle\langle\mathbf{p},r|\alpha_\mu e^{-i\mathbf{k}\cdot\mathbf{x}}|\mathbf{q},s\rangle\langle\mathbf{q},s|e^{i\mathbf{k}\cdot\mathbf{x}}\alpha^\mu|\mathbf{p}',r'\rangle\langle\mathbf{p}',r'|a\rangle}{E_{\mathbf{p},r}-E_{\mathbf{q},s}-k\ \mathrm{sgn}(E_{\mathbf{q},s})}.$$

For the numerical evaluation the expressions above can be expanded in partial waves.

b. Vertex correction

The first-order vertex correction (see Fig. 16) is in operator form represented by

$$\int\frac{dz}{2\pi}ie\alpha^{\mu'}iS_F(\omega'-z)ie\alpha^{\nu}A_\nu iS_F(\omega-z)ie\alpha^{\mu}iD_{F\mu'\mu}(z)=ie\Lambda^{(1)\nu}(\omega',\omega)A_\nu. \tag{C2}$$

Using the Feynman gauge, the coordinate representation becomes

$$\langle\mathbf{x}_2|i\Lambda^{(1)\nu}(\omega',\omega)|\mathbf{x}_1\rangle=4\pi\alpha\int\frac{dz}{2\pi}\int\frac{d^3k}{(2\pi)^3}\sum_{t,u}\frac{\alpha_\mu e^{-i\mathbf{k}\cdot\mathbf{x}_2}|u\rangle\langle u|\alpha^\nu|t\rangle\langle t|e^{i\mathbf{k}\cdot\mathbf{x}_1}\alpha^\mu}{(\omega'-z-E_u+i\eta_u)(\omega-z-E_t+i\eta_t)(z^2-\mathbf{k}^2+i\eta)}.$$

It then follows that

$$\frac{\partial}{\partial\omega}\Sigma^{(1)}_{bou}(\omega)=\Lambda^{(1)0}(\omega,\omega)_{diag},$$

where the subscript ''diag'' indicates the diagonal part of the vertex function with $t=u$. This is a general form of the Ward identity.

Integration over z gives (for simplicity restricting ourselves to *positive* intermediate energies)

$$\langle\mathbf{x}_2|i\Lambda^{(1)\nu}(\omega',\omega)|\mathbf{x}_1\rangle=-2\pi\alpha i\int\frac{d^3k}{(2\pi)^3}\frac{1}{k}\sum_{t,u}\frac{\alpha_\mu e^{-i\mathbf{k}\cdot\mathbf{x}_2}|u\rangle\langle u|\alpha^\nu|t\rangle\langle t|e^{i\mathbf{k}\cdot\mathbf{x}_1}\alpha^\mu}{(\omega'-E_u-k)(\omega-E_t-k)}.$$

The corresponding energy contribution is then

$$\begin{aligned}E^{(2)}_{vert}&=i\langle a|i\Lambda^{(1)\nu}(\omega',\omega)A_\nu|a\rangle\\&=2\pi\alpha\int\frac{d^3k}{(2\pi)^3}\frac{1}{k}\sum_{t,u}\frac{\langle a|\alpha_\mu e^{-i\mathbf{k}\cdot\mathbf{x}_2}|u\rangle\langle u|\alpha^\nu A_\nu|t\rangle\langle t|e^{i\mathbf{k}\cdot\mathbf{x}_1}\alpha^\mu|a\rangle}{(\omega'-E_u-k)(\omega-E_t-k)}.\end{aligned}$$

2. Second-order

We consider now the second-order self-energy diagrams in Figs. 17(g-i).

a. Diagram (g)

The two-photon self-energy diagram in Fig. 17(g) is represented by the operator ($E_a=E_b$)

$$\int\frac{dz'}{2\pi}\int\frac{dz}{2\pi}ie\alpha^{\nu'}iS_F(E_a-z')ie\alpha^{\mu'}iS_F(E_a-z-z')ie\alpha^\nu iS_F(E_a-z)ie\alpha^\mu iD_{F\nu'\nu}(z')iD_{F\mu'\mu}(z).$$

With the vertex correction, Eq. (C2), this amplitude becomes (see Fig. 18)

$$\int\frac{dz}{2\pi}ie\Lambda^{(1)\mu'}(E_a,E_a-z)iS_F(E_a-z)ie\alpha^\mu iD_{F\mu'\mu}(z).$$

This is the same as the first-order self-energy operator $i\Sigma^{(1)}(E_a)$ with $\alpha^{\mu'}$ replaced by $\Lambda^{(1)\mu'}$. Performing the z integrations, yields for positive intermediate energies the energy contribution

$$\Delta E^{(2)}_g=4\pi^2\alpha^2\int\frac{d^3k'}{(2\pi)^3}\frac{1}{k'}\int\frac{d^3k}{(2\pi)^3}\frac{1}{k}\sum_{t,u,v}\frac{\langle a|\alpha_\nu e^{-i\mathbf{k}'\cdot\mathbf{x}}|v\rangle\langle u|\alpha^\nu e^{i\mathbf{k}'\cdot\mathbf{x}}|t\rangle\langle v|\alpha_\mu e^{-i\mathbf{k}\cdot\mathbf{x}}|u\rangle\langle t|\alpha^\mu e^{i\mathbf{k}\cdot\mathbf{x}}|a\rangle}{(E_a-k'-E_v)(E_a-k-k'-E_u)(E_a-k-E_t)}-\text{mass counterterm}.\tag{C3}$$

The corresponding expressions for negative intermediate energies can be derived in a similar way but are not given here. The mass-counterterm can be evaluated in complete analogy with the corresponding first-order term in Eq. (C1) (see Fig. 13).

b. Diagram (h)

After mass-renormalizing the inner part, diagram (h) in Fig. 17 can be represented by the diagram in Fig. 19 and in operator form by

$$\int\frac{dz}{2\pi}ie\alpha^{\mu'}iS^{bou}_F(E_a-z)i\Sigma^{mass\text{-}ren(1)}_{bou}(E_a-z)iS^{bou}_F(E_a-z)ie\alpha^\mu iD_{F\nu'\nu}(z).$$

This is the same as the vertex correction, $i\Lambda^{(1)0}$, with the potential replaced by the renormalized self-energy operator, $\Sigma^{mass\text{-}ren(1)}_{bou}(E_a-z)$. The z-integration yields the energy contribution for positive intermediate states

$$\Delta E^{(2)}_h=2\pi\alpha\int\frac{d^3k}{(2\pi)^3}\frac{1}{k}\sum_{t,v}\frac{\langle a|\alpha_\mu e^{-i\mathbf{k}\cdot\mathbf{x}}|v\rangle\langle v|\Sigma^{mass\text{-}ren(1)}_{bou}(E_a-k)|t\rangle\langle t|\alpha^\mu e^{i\mathbf{k}\cdot\mathbf{x}}|a\rangle}{(E_a-E_v-k)(E_a-E_t-k)}-(\text{mass counterterm}).\tag{C4}$$

The mass counterterm can be evaluated in analogy with the previous cases, Eqs. (C1) and (C3) (see also Fig. 13).

c. Diagram (i)

Using the first-order self-energy operator, Eq. (C1), the energy contribution of the irreducible or nondegenerate part of diagram (i) in Fig. 17 can be expressed as

$$\Delta E_i^{(2)} = \sum_{E_u \neq E_a} \frac{\langle a|\Sigma_{bou}^{mass\text{-}ren(1)}(E_a)|u\rangle\langle u|\Sigma_{bou}^{mass\text{-}ren(1)}(E_a)|a\rangle}{E_a - E_u}.$$

The reducible or degenerate case $E_u = E_a$ leads, together with the product of the first-order diagrams, to the derivative term (see Appendix B)

$$\Delta E_i^{(2)'} = \langle a|\Sigma_{bou}^{mass\text{-}ren(1)}(E_a)|a\rangle \left\langle a \left| \left\{ \frac{\partial}{\partial \omega} \Sigma_{bou}^{mass\text{-}ren(1)}(\omega) \right\}_{\omega = E_a} \right| a \right\rangle.$$

3. The infrared divergences

The expressions for the individual second-order diagrams are infrared divergent, but the sum of the three diagrams is convergent, as can be shown as follows.

We consider the diagrams above for the case $E_t = E_v = E_a$ and E_u being positive (leaving out trivial constants and integrations), which for the mass-unrenormalized parts leads to

$$\Delta E_g^{(2)} \propto \frac{\langle a|\alpha_\nu e^{-i\mathbf{k}'\cdot\mathbf{x}}|a\rangle\langle u|\alpha^\nu e^{i\mathbf{k}'\cdot\mathbf{x}}|a\rangle\langle a|\alpha_\mu e^{-i\mathbf{k}\cdot\mathbf{x}}|u\rangle\langle a|\alpha^\mu e^{i\mathbf{k}\cdot\mathbf{x}}|a\rangle}{E_a - E_u - k - k'}, \tag{C5}$$

$$\Delta E_h^{(2)} \propto \frac{k'}{k} \frac{\langle a|\alpha_\mu e^{-i\mathbf{k}\cdot\mathbf{x}}|a\rangle\langle a|\alpha^\mu e^{i\mathbf{k}\cdot\mathbf{x}}|a\rangle\langle a|\alpha_\nu e^{-i\mathbf{k}'\cdot\mathbf{x}}|u\rangle\langle u|\alpha^\nu e^{i\mathbf{k}'\cdot\mathbf{x}}|a\rangle}{E_a - E_u - k - k'},$$

$$\Delta E_i^{(2)'} \propto -\frac{k'}{k} \frac{\langle a|\alpha_\nu e^{-i\mathbf{k}'\cdot\mathbf{x}}|u\rangle\langle u|\alpha^\nu e^{i\mathbf{k}'\cdot\mathbf{x}}|a\rangle}{E_a - E_u - k'} \langle a|\alpha_\mu e^{-i\mathbf{k}\cdot\mathbf{x}}|a\rangle\langle a|\alpha^\mu e^{i\mathbf{k}\cdot\mathbf{x}}|a\rangle.$$

The last two contributions are logarithmically divergent, when $k \to 0$, but the sum of them,

$$\Delta E_h^{(2)} + \Delta E_i^{(2)'} \propto k' \frac{\langle a|\alpha_\mu e^{-i\mathbf{k}\cdot\mathbf{x}}|a\rangle\langle a|\alpha^\mu e^{i\mathbf{k}\cdot\mathbf{x}}|a\rangle\langle a|\alpha_\nu e^{-i\mathbf{k}'\cdot\mathbf{x}}|u\rangle\langle u|\alpha^\nu e^{i\mathbf{k}'\cdot\mathbf{x}}|a\rangle}{(E_a - E_u - k')(E_a - E_u - k - k')},$$

is convergent for $E_u \neq E_a$. For $E_u = E_a$ this expression is still divergent but is exactly cancelled by the first contribution (C5). Therefore, the sum of all three energy contributions is infrared convergent. In a similar way it can be shown that the corresponding mass counterterms cancel.

APPENDIX D: CHARGE DIVERGENCES

In this appendix we show that the charge divergences of the diagrams in Figs. 17(g-i) cancel.

1. Zero- and one-potential terms

The free-electron self-energy in the momentum representation can generally be expressed as

$$\Sigma_{free}(p) = A + B(\not{p} - m) + C(\not{p} - m)^2, \tag{D1}$$

where

$$A = |\Sigma_{free}(p)|_{\not{p}=m}$$

and

$$B = \left| \frac{\partial}{\partial \not{p}} \Sigma_{free}(p) \right|_{\not{p}=m}.$$

A and B are logarithmically divergent constants and associated with the mass and charge divergence, respectively. The last term is finite and represents the mass- and charge-renormalized free-electron self-energy.

Each diagram of the free-electron self-energy operator contains in the momentum representation one or several free-electron propagators of the type (see Appendix A)

$$S_F^{free}(p) = \frac{1}{\omega - h^{free}} = \frac{1}{\omega - (\boldsymbol{\alpha}\cdot\mathbf{p} + \beta m)} = \frac{1}{\not{p} - m}\beta.$$

In the corresponding bound self-energy, the free-electron propagators are replaced by the bound-state propagators

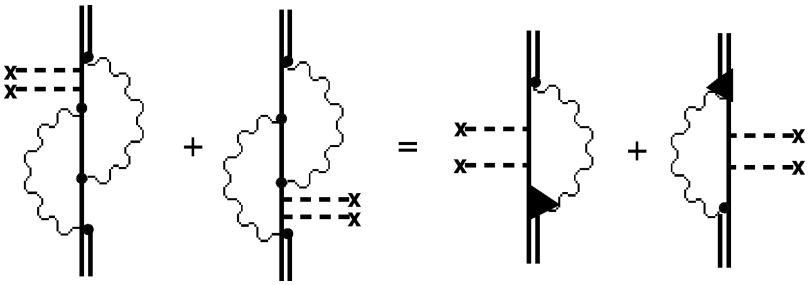

FIG. 20. Charge divergences in the diagram 17(g).

$$S_F^{bou}(p)=\frac{1}{\omega-h^{bou}}=\frac{1}{\omega-(\boldsymbol{\alpha}\cdot\mathbf{p}+\beta m+V)}=\frac{1}{\not p-m-\beta V}\beta.$$

It then follows that we can expand the bound self-energy in terms of the free-electron self-energy and its derivatives in the following way:

$$\begin{aligned}\Sigma_{bou}(p)&=\Sigma_{free}(p)-V\frac{\partial}{\partial\omega}\Sigma_{free}(p)\\&\quad+\frac{1}{2}V^2\frac{\partial^2}{\partial\omega^2}\Sigma_{free}(p)-\cdots\\&=\Sigma_{free}(p)-\beta V\frac{\partial}{\partial\not p}\Sigma_{free}(p)\\&\quad+\frac{1}{2}V^2\frac{\partial^2}{\partial\not p^2}\Sigma_{free}(p)-\cdots.\end{aligned}$$

The first term represents the self-energy with internal free-electron lines, the second term the same with one potential interaction in all possible places, etc.

The free-electron self-energy $\Sigma_{free}(p)$ contains a charge divergent part, $B(\not p-m)$. When operating on a bound state $|a\rangle$, we have

$$\begin{aligned}(\hat{\not p}-m)|a\rangle&=(\hat{\not p}-m)|p\rangle\langle p|a\rangle\\&=\beta(p_0-\boldsymbol{\alpha}\cdot\hat{\mathbf{p}}-\beta m)|p\rangle\langle p|a\rangle\\&=\beta(p_0-\hat h^{bou}+V)|a\rangle.\end{aligned}$$

Thus, for $p_0=\omega=E_a$,

$$B(\hat{\not p}-m)|a\rangle=B\beta V|a\rangle.$$

But

$$\frac{\partial}{\partial\omega}\Sigma_{free}(p)=\beta B+(\text{finite part}),$$

which implies that—for a bound self-energy operator acting on the energy shell ($p_0=\omega=E_a$)—the charge divergence of the first two terms of the expansion cancel or, in other words, that *the charge divergence of diagrams with zero and one potential interaction generally cancel*. Thus, the diagram is charge divergent only to the extent that the corresponding diagrams with free-electron lines with two or more potential interactions are divergent. In first order it is well-known that the free-electron self-energy diagram with two potential interactions is finite, and hence the first-order bound self-energy is free from charge divergence, when acting on the energy shell.

2. Multipotential terms

a. Diagram (g)

We shall now consider the diagrams (g-i) in Fig. 17 specifically and show that the charge divergences of the three diagrams cancel. Performing a potential expansion of the bound-state propagators, we know that the charge divergences of the zero- and one-potential terms cancel. Remaining to be considered are the two-potential terms. In diagram (g) the only possible divergence lies in the diagrams given in Fig. 20. If we include also the remaining parts of the potential expansion (after eliminating the cancelling charge-divergent parts of the zero- and one-potential interactions), we can express this after mass renormalization as the diagrams in Fig. 21.

The vertex function involved here, $\Lambda^{(1)0}(E_a,E_a-z)$, contains a divergent part, βB, as follows from the Ward-Takahashi theorem [20],

$$\begin{aligned}(p-p')^\mu\Lambda_\mu(p,p')&=\not p-\not p'+\Sigma_{free}(p')-\Sigma_{free}(p)\\&=B(\not p-\not p')+(\text{finite part}).\end{aligned}$$

Hence, the charge-divergent part of diagram (g) is $2\beta B$ times the first-order mass-renormalized self-energy

$$\Delta E_g^{charge\text{-}div}=2\beta B\langle a|-\Sigma_{bou}^{mass\text{-}ren(1)}(E_a)|a\rangle.$$

b. Diagram (h)

The diagram (h) in Fig. 17 can be expanded as shown in Fig. 22, leaving out the finite many-potential term. The zero-potential part is represented by the Feynman amplitude

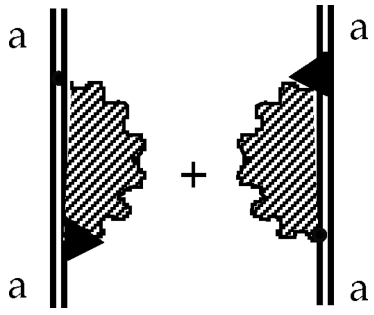

FIG. 21. Diagram 17(g) renormalized.

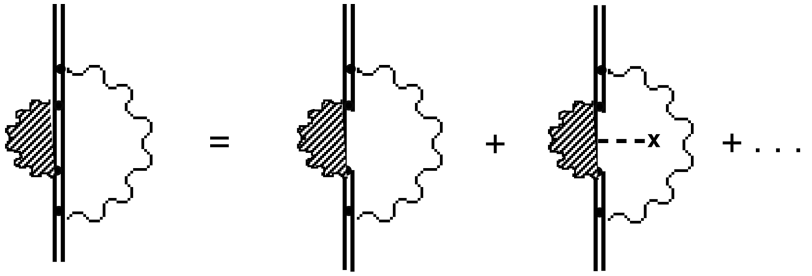

FIG. 22. Potential expansion of the self-energy modified propagator contribution.

$$\left\langle a\left|\int\frac{dz}{2\pi}ie\alpha^{\mu'}iS_F^{bou}(E_a-z)i\Sigma_{free}^{mass\text{-}ren(1)}(E_a-z)iS_F^{bou}(E_a-z)ie\alpha^{\mu}iD_{F\mu'\mu}(z)\right|a\right\rangle.$$

Using Eq. (D1), the charge-divergent part of this amplitude becomes

$$\left\langle a\left|\int\frac{dz}{2\pi}ie\alpha^{\mu'}iS_F^{bou}(E_a-z)iB(\hat{\boldsymbol{p}}-m)iS_F^{bou}(E_a-z)ie\alpha^{\mu}iD_{F\mu'\mu}(z)\right|a\right\rangle \tag{D2}$$

with $p_0=E_a-z$. But with the form of the bound-state propagator given in Sec. III we have

$$\begin{aligned}(\hat{\boldsymbol{p}}-m)S_F^{bou}(E_a-z)&=\beta(E_a-z-\hat{h}^{bou}+V)\frac{1}{E_a-z-\hat{h}^{bou}}\\&=\beta[1+VS_F^{bou}(E_a-z)],\end{aligned} \tag{D3}$$

and it can then be shown that the second term in Eq. (D3) gives rise to a contribution that is exactly cancelled by the one-potential diagram. Since the many-potential term is finite, the remaining charge divergence of the Feynman amplitude becomes

$$\left\langle a\left|\int\frac{dz}{2\pi}ie\alpha^{\mu'}iS_F^{bou}(E_a-z)i^2\beta Bie\alpha^{\mu}iD_{F\mu'\mu}(z)\right|a\right\rangle=-i\beta B\langle a|\Sigma^{bou}(E_a)|a\rangle.$$

The corresponding energy contribution is then

$$\Delta E_h^{charge\text{-}div}=\beta B\langle a|\Sigma^{bou}(E_a)|a\rangle.$$

A similar analysis of the mass-renormalization term in Fig. 13 leads to the charge-divergent energy contribution

$$\beta B\langle a|p\rangle\langle p|\Sigma^{free}(E_a)|p\rangle\langle p|a\rangle=\beta B\langle a|\Sigma_{counter}^{mass}|a\rangle,$$

using Eq. (4.2). This removes the mass divergence from the expression (D2), and the final result for the charge-divergent part of diagram (h) after mass-renormalization becomes

$$\Delta E_{h(mass\text{-}ren)}^{charge\text{-}div}=\beta B\langle a|\Sigma_{bou}^{mass\text{-}ren(1)}(E_a)|a\rangle.$$

c. Diagram (i)

The charge divergence of diagram (i) in Fig. 17 comes from the reference-state contribution (4.1)

$$\begin{aligned}\Delta E_i=&\langle a|-\Sigma_{bou}^{mass\text{-}ren(1)}(E_a)|a\rangle\\&\times\left\langle a\left|\left\{\frac{\partial}{\partial\omega}[-\Sigma_{bou}^{mass\text{-}ren(1)}(\omega)]\right\}_{\omega=E_a}\right|a\right\rangle.\end{aligned}$$

The first matrix element is free from charge divergence, according to the discussion above. The derivative contains a charge-divergent part βB from the free component. The remaining parts are finite. Therefore, the charge-divergent part of diagram (i) is

$$\Delta E_i^{charge\text{-}div}=\beta B\langle a|\Sigma_{bou}^{mass\text{-}ren(1)}(E_a)|a\rangle.$$

This completes the proof that the charge divergences of the three diagrams cancel.

[1] See, for instance, J. Sapirstein and D.R. Yennie, in *Quantum Electrodynamics*, edited by T. Kinoshita (World Scientific, Singapore, 1990); *The Hydrogen Atom*, edited by G.F. Bassani, M. Inguscio, and T.W. Hänsch (Springer-Verlag, Berlin, 1989); M. Boshier, in *Proceedings of the Fifteenth International Conference on Atomic Physics*, edited by H. B. Van Linden Van Den Heuvell, J. T. M. Walraven, and M. W. Reynolds (World Scientific, Singapore, 1996), pp. 328–342; M. Weitz *et al.*, Phys. Rev. A **52**, 2664 (1995).

[2] K. Pachucki, Phys. Rev. Lett. **72**, 3154 (1994); T. Kinoshita

and M. Nio, Phys. Rev. D **53**, 4909 (1996); S.G. Karshenboim, J. Phys. B **29**, L29 (1996).

[3] See, for instance, Heavy-Ion Spectroscopy and QED Effects in Atomic Systems, Proceedings of the Nobel Symposium 85, Saltsjöbaden, Sweden, 1992 [Phys. Scr. **T46** (1993)]; Trapped Particles and Related Fundamental Physics, Proceedings of the Nobel Symposium 91, Lysekil, Sweden, 1994 [*ibid.* **T59** (1995)].

[4] H.F. Beyer *et al.*, Z. Phys. D **35**, 168 (1995).

[5] P.J. Mohr, Phys. Rev. A **46**, 4421 (1992); P.J. Mohr and G. Soff, Phys. Rev. Lett. **70**, 158 (1993).

[6] H. Persson, I. Lindgren, L.N. Labzowsky, G. Plunien, T. Beier, and G. Soff, Phys. Rev. A **54**, 2805 (1996).

[7] H. Persson, I. Lindgren, S. Salomonson, and P. Sunnergren, Phys. Rev. A **48**, 2772 (1993).

[8] T. Beier and G. Soff, Z. Phys. D **8**, 129 (1988); S.M. Schneider, W. Greiner, and G. Soff, J. Phys. B **26**, L529 (1993); G. Plunien, T. Beier, H. Persson, and G. Soff, Z. Phys. (to be published).

[9] I. Lindgren, H. Persson, S. Salomonson, V. Karasiev, L. Labzowsky, A. Mitrushenkov, and M. Tokman, J. Phys. B **26**, L503 (1993).

[10] S. Mallampalli and J. Sapirstein, Phys. Rev. A **54**, 2714 (1996).

[11] S.A. Blundell and N.J. Snyderman, Phys. Rev. A **44**, R1427 (1991).

[12] S.A. Blundell, Phys. Rev. A **46**, 3762 (1992).

[13] I. Lindgren, H. Persson, S. Salomonson, and A. Ynnerman, Phys. Rev. A **47**, R4555 (1993).

[14] I. Lindgren, H. Persson, S. Salomonson, and L. Labzowsky, Phys. Rev. A **51**, 1167 (1995).

[15] H. Persson, S. Salomonson, P. Sunnergren, and I. Lindgren, Phys. Rev. Lett. **76**, 204 (1996).

[16] H.M. Quiney and I.P. Grant, J. Phys. B **27**, L199 (1994).

[17] L.N. Labzowsky and A.O. Mitrushenkov, Phys. Rev. A **53**, 3029 (1996); Phys. Lett. A **198**, 333 (1995).

[18] A. Mitrushenkov, L. Labzowsky, I. Lindgren, H. Persson, and S. Salomonson, Phys. Lett. A **200**, 51 (1995).

[19] S. Mallampalli and J. Sapirstein, Phys. Rev. A **57**, 1548 (1998).

[20] C. Itzykson and J.-B. Zuber, *Quantum Field Theory* (McGraw-Hill, New York, 1980); F. Mandl and S. Shaw, *Quantum Field Theory* (John Wiley and Sons Ltd., New York, 1985).

[21] J.A. Fox and D.R. Yennie, Ann. Phys. (N.Y.) **81**, 438 (1973).

[22] M. Gell-Mann and F. Low, Phys. Rev. **84**, 350 (1951); J. Sucher, Phys. Rev. **107**, 1448 (1957).

[23] H. Persson, S. Salomonson, and P. Sunnergren, in Proceedings of Modern Trends in Atomic Physics, edited by H. Persson and D. Hanstorp [Adv. Quantum Chem. **30**, 379 (1998)].